Imaging Science in Dentistry 2015; 45: 15-22
http://dx.doi.org/10.5624/isd.2015.45.1.15

Reproducibility of the sella turcica landmark in three dimensions using a sella turcica-specific reference system

Pisha Pittayapat[1,2,*], Reinhilde Jacobs[1], Guillaume A. Odri[3], Karla de Faria Vasconcelos[4], Guy Willems[5], Raphaël Olszewski[6]

[1]*OIC, OMFS-IMPATH Research Group, Department of Imaging and Pathology, Faculty of Medicine, University of Leuven and Oral and Maxillofacial Surgery, University Hospitals Leuven, Leuven, Belgium*

[2]*Department of Radiology, Faculty of Dentistry, Chulalongkorn University, Bangkok, Thailand*

[3]*Service de Chirurgie Orthopédique et Traumatologique, Centre Hospitalier Régional d'Orléans, Orléans Cedex 2, France*

[4]*Department of Oral Diagnosis, Division of Oral Radiology, Piracicaba Dental School, University of Campinas, Piracicaba, São Paulo, Brazil*

[5]*Orthodontics, Department of Oral Health Sciences, KU Leuven and Dentistry, University Hospitals Leuven, University of Leuven, Leuven, Belgium*

[6]*Department of Oral and Maxillofacial Surgery, Cliniques Universitaires Saint Luc, Université Catholique de Louvain, Brussels, Belgium*

ABSTRACT

Purpose: This study was performed to assess the reproducibility of identifying the sella turcica landmark in a three-dimensional (3D) model by using a new sella-specific landmark reference system.

Materials and Methods: Thirty-two cone-beam computed tomographic scans (3D Accuitomo® 170, J. Morita, Kyoto, Japan) were retrospectively collected. The 3D data were exported into the Digital Imaging and Communications in Medicine standard and then imported into the Maxilim® software (Medicim NV, Sint-Niklaas, Belgium) to create 3D surface models. Five observers identified four osseous landmarks in order to create the reference frame and then identified two sella landmarks. The *x*, *y*, and *z* coordinates of each landmark were exported. The observations were repeated after four weeks. Statistical analysis was performed using the multiple paired t-test with Bonferroni correction (intraobserver precision: $p<0.005$, interobserver precision: $p<0.0011$).

Results: The intraobserver mean precision of all landmarks was <1 mm. Significant differences were found when comparing the intraobserver precision of each observer ($p<0.005$). For the sella landmarks, the intraobserver mean precision ranged from 0.43 ± 0.34 mm to 0.51 ± 0.46 mm. The intraobserver reproducibility was generally good. The overall interobserver mean precision was <1 mm. Significant differences between each pair of observers for all anatomical landmarks were found ($p<0.0011$). The interobserver reproducibility of sella landmarks was good, with $>50\%$ precision in locating the landmark within 1 mm.

Conclusion: A newly developed reference system offers high precision and reproducibility for sella turcica identification in a 3D model without being based on two-dimensional images derived from 3D data. (***Imaging Sci Dent 2015; 45: 15-22***)

KEY WORDS: Cephalometry; Cone-Beam Computed Tomography; Orthodontics; Sella Turcica; Imaging, Three-Dimensional

Introduction

Cephalometric analysis is an essential part of orthodontic treatment planning. Each analysis involves assessing several cephalometric landmarks. Superimposing structures onto a lateral cephalogram is a technique used to perform

*This work was supported by a doctoral scholarship in the framework of the Inter-faculty Council for Development Co-operation (IRO).
Received August 4, 2014; Revised October 16, 2014; Accepted November 3, 2014
*Correspondence to : Dr. Pisha Pittayapat
OIC, OMFS-IMPATH Research Group, Department of Imaging and Pathology, Faculty of Medicine, University of Leuven and Oral and Maxillofacial Surgery, University Hospitals Leuven, Kapucijnenvoer 7, Leuven 3000-Belgium
Tel) 32-16-34-1975, Fax) 32-16-33-2410, E-mail) p.pittayapat@gmail.com

an individual's longitudinal growth evaluation and to assess the outcome of orthodontic treatment.

The sella turcica landmark is one of the most commonly used cephalometric landmarks, and is located at the center of the pituitary fossa in the cranial base. The morphology of the sella turcica has been described by several authors.[1-7] Variations in the shape and size of the sella turcica in adults have been described in the literature.[4] The sella turcica can be classified into three segments: the anterior wall, the floor, and the posterior wall (dorsum sellae). Its shape can be round, oval, or flat, with the oval type being the most common.[5]

Traditionally, cephalometric tracing is performed on a lateral cephalogram, a technique that was first introduced by Hofrath[8] in Germany and Broadbent[9] in the United States. Although this technique was widely accepted as a standard tool for orthodontic treatment planning for several decades, it has shown several disadvantages because of the geometric distortion and superimposition of structures on the radiographs.

Recently, three-dimensional (3D) imaging modalities such as computed tomography (CT) and cone-beam computed tomography (CBCT) have played an important role in dentistry. CBCT requires relatively lower radiation doses than multi-slice CT,[10] and has therefore become very popular for maxillofacial diagnosis and treatment planning. 3D images allow orthodontists to visualize craniofacial structures in three dimensions without involving the superimposition of anatomical structures.[11-13] This modality has proven to be useful in several orthodontic applications, including 3D cephalometry.

3D cephalometry offers orthodontists the opportunity to identify cephalometric landmarks in three dimensions with the aid of 3D image viewing software.[14,15] Several publications have that this technique has advantages over traditional two-dimensional (2D) cephalometric analysis, especially regarding the accuracy of the measurements[16,17] and the reproducibility of landmark identification.[18-20]

In 3D maxillofacial software, the sella point is usually identified based on 2D cephalometric images generated from 3D data, either from CT or CBCT.[14] Previously published reports have indicated that this technique led to satisfactory identification of the sella point;[21-23] however, it has been proposed that the sella landmark identified on the generated 2D image may not truly corresponds to the real geometric center of the sella turcica, especially in situations where the shape of the sella turcica is not within the normal range. No reliable method of identifying the sella point, which is a floating landmark in nature, on real 3D surface models has been published.[20] Therefore, the aim of this study was to assess the reproducibility of a new technique to identify the sella landmark in a 3D model by using a newly developed reference system.

Materials and Methods

The study protocol (reference number: ML6960, BE 322201010078) was approved by the Medical Ethics Committee of the University Hospitals Leuven. The authors have read the Helsinki Declaration and have followed its guidelines in this investigation.

Thirty-two patients (11 males and 21 females, age range 8.8-76.7 years, mean age 26.0 ± 21.6 years) were retrospectively selected from the hospital database. The selection criteria were: (1) patients with CBCT images, (2) the presence of the sella turcica in the images, (3) no significant pathology of the maxillofacial region, (4) no significant facial asymmetry, and (5) no significant anatomical variation in the sella turcica and sphenoidal regions.

The CBCT scans of each patient were taken with a 3D Accuitomo® 170 device (J. Morita, Kyoto, Japan) with a minimum field of view of 140 × 100 mm (90 kVp, 154 mAs, voxel size 0.25 mm.) The CBCT data were exported from the i-Dixel® software (J. Morita, Kyoto, Japan) into the Digital Imaging and Communications in Medicine format and then imported into the Maxilim® software (Medicim NV, Sint-Niklaas, Belgium). Three-dimensional surface models for all subjects were created using the full CBCT volume with 0.5-mm voxel subsampling. The threshold value was set between 276 and 476 in order to segment the hard tissues for the 3D models. The models were then saved and randomized.

Reference frame

A reference system was created in the Maxilim® software in order to identify the geometric center or midpoint of the sella turcica. The reference frame was composed of six landmarks (four operator-indicated landmarks and two software-calculated landmarks) and two sella landmarks, which were indicated on two distinct vertical planes created from the reference system (Table 1) (Fig. 1).

Image evaluation

Five observers (two third-year orthodontic residents, two dentomaxillofacial radiologists with five and eight years

Table 1. Landmarks used in this reference system and their definitions

Landmark	Definition
Anterior clinoid process, right (ACP-R)	The tip of the anterior clinoid process on the right side
Anterior clinoid process, left (ACP-L)	The tip of the anterior clinoid process on the left side
Apex of the petrous part of the temporal bone, right (APT-R)	The apex of the petrous part of the temporal bone on the right side
Apex of the petrous part of the temporal bone, left (APT-L)	The apex of the petrous part of the temporal bone on the left side
Mid-ACP	A point halfway between the ACP-R and ACP-L, as indicated by the software
Mid-APT	A point halfway between the APT-R and APT-L, as indicated by the software
Sella turcica on a plane through the mid-ACP (Sella 1)	The sella turcica identified on a vertical plane passing through the mid-ACP and perpendicular to a plane created by the mid-ACP, APT-R, and APT-L
Sella turcica on a plane through the mid-APT (Sella 2)	The sella turcica identified on a vertical plane passing through the mid-APT and perpendicular to a plane created by the mid-APT, ACP-R, and ACP-L

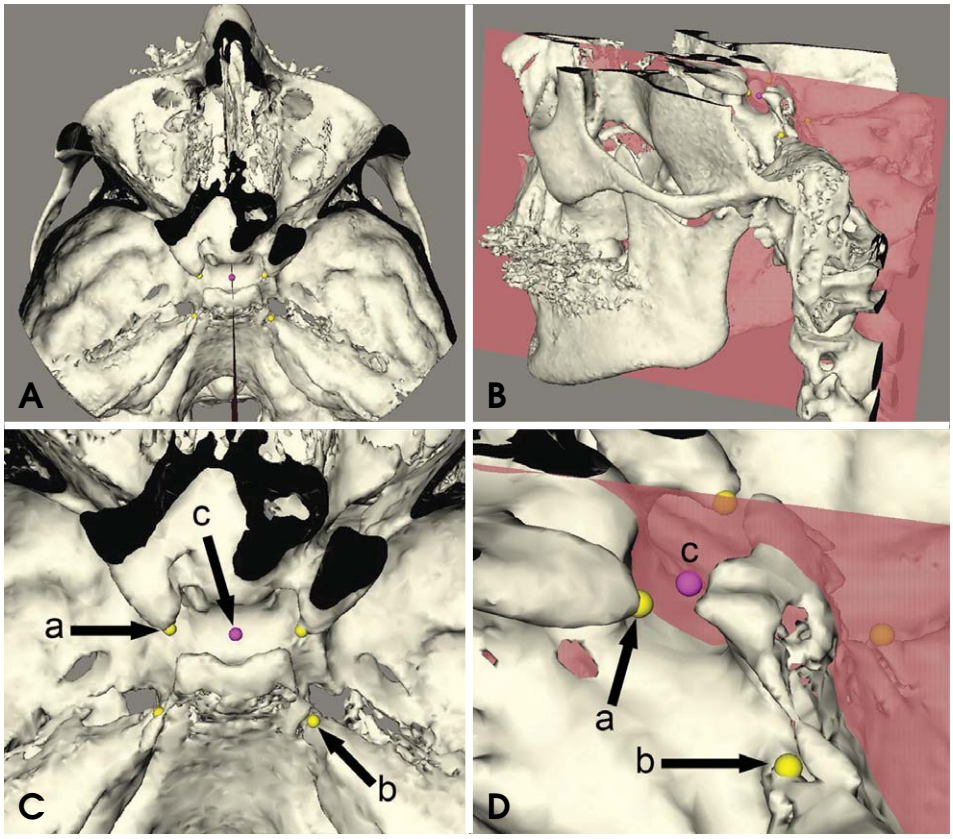

Fig. 1. (A) and (B) show a three-dimensional model of one patient in a top and oblique overview, respectively. In this figure, a reference system is created by locating four landmarks (the right and left anterior clinoid process [ACP] and the right and left apex of the petrous part of the temporal bone right [APT]). (C) is a close-up of the top view presented in (A), showing the landmarks that form the reference system: (a) right and left ACP, (b) right and left APT, and (c) one of the sella landmarks. (D) is a close-up of the oblique view, showing landmarks (a), (b), and (c). The sella landmark (c) was located on one of the vertical planes created from the reference system in the Maxilim® software.

of experience, respectively, and one maxillofacial surgeon with 20 years of experience) were initially introduced to the technique through an instruction and calibration session that allowed the observers to understand the definitions of the landmarks and to become familiar with the software.

During each observation session, an observer identified six landmarks (Table 1). The *x*, *y*, and *z* coordinates of each landmark were exported to Microsoft Excel files. Another observation session was conducted four weeks later to obtain data about intraobserver precision and reproducibility.

Statistical analysis

The *x*, *y*, and *z* coordinates of six landmarks (four operator-indicated landmarks in the reference system and two sella landmarks) were exported and entered into Microsoft Excel (Microsoft Corp., Redmond, WA, USA). For each pair of landmarks identified by the observers, the Euclidean distance *d* between the two points was calculated by the

formula:

$$d=\sqrt{\{(x_1-x_2)^2+(y_1-y_2)^2+(z_1-z_2)^2\}}$$

The coordinates (x_1, y_1, z_1) indicate the coordinates at time point 1 or the coordinates from observer 1, depending on the context. Likewise, the coordinates (x_2, y_2, z_2) indicate the coordinates at time point 2 or the coordinates from observer 2, depending on the context. The same convention was used for indicating the coordinates from observers 3-5.

In this study, precision was defined for a given landmark as the mean distance of the coordinates of that landmark on all subjects as reported by all observers. Intraobserver precision was defined for a given landmark as the mean distance of all coordinates for that landmark on all subjects as reported by each observer. Interobserver precision was defined for a given landmark as the mean distance of all coordinates of that landmark on all subjects as reported by each pair of observers.

The reproducibility was defined in terms of the percentage of precision values falling within one of the following ranges: <0.5 mm, 0.5-1 mm, and >1 mm. These thresholds were used for both intraobserver and interobserver reproducibility.

Parametrical tests were used for statistical analysis, since the data were normally distributed.

Intraobserver precision

The multiple paired t-test with Bonferroni correction was performed on the transformed variable to assess the variation of intraobserver precision for each landmark across observers. Analysis of variation (ANOVA) with Tukey's post-hoc test was used to compare the mean values of intraobserver precision across landmarks for each observer.

Interobserver precision

All the possible distances between pairs of two points observed by each pair of observers were calculated, resulting four distance values in total for each subject and each landmark.

The multiple paired t-test with Bonferroni correction ($p<0.0083$) was performed to compare the four distances described above. None of the comparisons indicated statistical significance. Therefore, the distances were joined together and different time points were not taken into account.

The mean precision values for each landmark as assessed by each pair of observers were evaluated by the multiple paired t-test with Bonferroni correction. ANOVA with Tukey's post-hoc test was calculated to compare the precision values among landmarks corresponding to the values obtained by each pair of observers.

Results

The results showed that all distances were positive and normally distributed.

Intraobserver precision and reproducibility

The intraobserver precision results are shown in Table 2. The mean intraobserver precision for all landmarks was <1 mm. The best mean precision was 0.23 ± 0.39 mm for the left anterior clinoid process (ACP-L). The poorest mean precision was 0.96 ± 1.76 mm for the right apex of the petrous part of the temporal bone (APT-R). For the sella turcica landmarks (Sella 1 and Sella 2), the mean intraobserver precision ranged from 0.35 ± 0.37 mm to 0.55 ± 0.45 mm.

Comparing the intraobserver precisions of each observer, using the multiple paired t-test with Bonferroni correction on the transformed variable, showed significant differences ($p<0.005$) for ACP-R, ACP-L, and APT-L. This implies that some observers were able to identify the ACP-R, ACP-L, and APT-L with significantly greater accuracy than others.

Statistically significant differences were found for the APT-R and APT-L when analyzing the intraobserver precision results for each observer across all landmarks (ANOVA with Tukey's post-hoc test, $p<0.05$). These results indicate that most observers identified the APT-R and APT-L with poorer precision than other landmarks.

The intraobserver reproducibility of landmarks (Table 3) was generally good, with $>50\%$ of mean distance values <1 mm. However, in one observer, 53.1% of the precision values for the APT-L were >1 mm. Sella 1 and Sella 2 showed good intraobserver reproducibility for all observers, with only 6.3-15.6% of mean distances >1 mm (Table 3).

Interobserver precision and reproducibility

The interobserver precision results are shown in Table 4. For most landmarks, the interobserver mean precision was <1 mm except for the APT-R and APT-L, the mean precision of which was >1 mm for most pairs of observers.

Significant differences were found between each pair of

Table 2. Intraobserver precision (mm, mean ± SD)

	Observer 1	Observer 2	Observer 3	Observer 4	Observer 5
ACP-R	0.28 ± 0.35	0.36 ± 0.32	0.59 ± 0.49	0.33 ± 0.44	0.46 ± 0.43
ACP-L	0.23 ± 0.39	0.30 ± 0.46	0.57 ± 0.50	0.37 ± 0.38	0.38 ± 0.42
APT-R	0.49 ± 0.74	0.60 ± 1.02	0.76 ± 1.38	0.96 ± 1.76	0.70 ± 1.06
APT-L	0.40 ± 0.83	0.45 ± 0.73	0.96 ± 1.24	0.82 ± 0.78	0.75 ± 1.02
Sella 1	0.49 ± 0.41	0.43 ± 0.34	0.51 ± 0.39	0.40 ± 0.40	0.42 ± 0.46
Sella 2	0.46 ± 0.38	0.55 ± 0.45	0.51 ± 0.46	0.35 ± 0.37	0.44 ± 0.43

Table 3. Reproducibility of intraobserver precision for each observer. Percentage of precision values < 0.5 mm, 0.5-1 mm, and > 1 mm

	Observer 1			Observer 2			Observer 3			Observer 4			Observer 5		
	< 0.5	0.5-1	> 1	< 0.5	0.5-1	> 1	< 0.5	0.5-1	> 1	< 0.5	0.5-1	> 1	< 0.5	0.5-1	> 1
ACP-R	75.0	18.75	6.25	71.88	28.13	0.00	31.25	53.13	15.63	71.88	15.63	12.50	59.38	25.00	15.63
ACP-L	75.00	18.75	6.25	62.50	34.38	3.13	40.63	37.50	21.88	59.38	37.50	3.13	68.75	21.88	9.38
APT-R	75.00	18.75	6.25	71.88	28.13	0.00	31.25	53.13	15.63	71.88	15.63	12.50	59.38	25.00	15.35
APT-L	59.38	21.88	18.75	56.25	28.13	15.63	25.00	21.88	53.13*	21.88	34.38	43.75	31.25	25.00	43.75
Sella 1	53.13	34.38	12.50	56.25	34.38	9.38	53.13	37.50	9.38	71.88	18.75	9.38	50.00	43.75	6.25
Sella 2	65.63	28.13	6.25	43.75	40.63	15.63	46.88	46.88	6.25	71.88	18.75	9.38	50.00	43.75	6.25

*> 50% of precision values > 1 mm

Table 4. Interobserver precision (mm) for each pair of observers (mean ± SD)

	ACP-R	ACP-L	APT-R	APT-L	Sella 1	Sella 2
O1/2	0.55 ± 0.55	0.44 ± 0.51	0.84 ± 1.46	0.62 ± 1.26	0.67 ± 0.53	0.63 ± 0.57
O1/3	0.45 ± 0.53	0.44 ± 0.47	0.79 ± 1.00	0.79 ± 1.17	0.68 ± 0.6	0.70 ± 0.61
O1/4	0.62 ± 0.57	0.66 ± 0.53	1.93* ± 1.89	1.58* ± 1.39	0.78 ± 0.63	0.76 ± 0.65
O1/5	0.44 ± 0.51	0.48 ± 0.52	0.88 ± 1.18	0.81 ± 1.03	0.76 ± 0.61	0.68 ± 0.6
O2/3	0.53 ± 0.57	0.53 ± 0.48	1.04* ± 1.12	0.87 ± 1.16	0.59 ± 0.48	0.62 ± 0.50
O2/4	0.59 ± 0.63	0.57 ± 0.54	1.62* ± 1.77	1.32* ± 1.19	0.53 ± 0.45	0.58 ± 0.51
O2/5	0.55 ± 0.55	0.47 ± 0.47	1.19* ± 1.30	1.03* ± 1.13	0.65 ± 0.53	0.65 ± 0.55
O3/4	0.64 ± 0.59	0.59 ± 0.53	1.82* ± 1.91	1.63* ± 1.53	0.66 ± 0.53	0.62 ± 0.52
O3/5	0.57 ± 0.53	0.56 ± 0.51	0.85 ± 1.06	0.98 ± 1.06	0.85 ± 0.69	0.56 ± 0.45
O4/5	0.45 ± 0.46	0.44 ± 0.46	1.99* ± 1.82	2.03* ± 1.71	0.71 ± 0.57	0.70 ± 0.55

*Mean precision >1 mm, O: observer

observers for all anatomical landmarks ($p < 0.0011$), implying that interobserver precision and reproducibility was observer-dependent.

For each pair of observers, ANOVA with Tukey's post-hoc test was also performed to compare the mean precision values across landmarks. It was found that for all pairs of observers, the ACP-R and ACP-L were observed with significantly better precision than other landmarks ($p < 0.05$). For most pairs of observers, Sella 1 and Sella 2 were observed with better precision than the APT-R and APT-L, and precision values for Sella 1 and Sella 2 were sometimes as good as those of the ACP-R and ACP-L ($p < 0.05$).

Table 5 shows interobserver reproducibility in terms of the percentage of values that fall into each of the following ranges: < 0.5 mm, 0.5-1 mm, and > 1 mm. The reproducibility was good to very good for the ACP-R and ACP-L (only 9.4%-30.5% of mean precision values > 1 mm). The reproducibility of the APT-R and APT-L was poorer (36.7%-90.6% of mean precision values > 1 mm). The reproducibility of the two sella turcica landmarks, Sella 1 and Sella 2, was shown to be good (7.8%-37.5% of mean precision values > 1 mm).

Discussion

The current study investigated the precision and reproducibility of the landmarks incorporated into a new reference system that was developed to facilitate the precise identification of the sella turcica landmark on 3D models.

Table 5. Interobserver reproducibility for each pair of observers. Percentages of precision values <0.5 mm, 0.5-1 mm and >1 mm

	ACP-R			ACP-L			APT-R			APT-L			Sella 1			Sella 2		
	<0.5	0.5-1	>1	<0.5	0.5-1	>1	<0.5	0.5-1	>1	<0.5	0.5-1	>1	<0.5	0.5-1	>1	<0.5	0.5-1	>1
O1/2	47.66	31.25	21.09	57.03	25.78	17.19	32.03	21.09	46.88	42.19	21.09	36.72	28.91	48.44	22.66	32.81	42.97	24.22
O1/3	57.03	25.78	17.19	50.78	39.84	9.38	28.13	35.16	36.72	28.91	27.34	43.75	28.13	46.88	25.00	25.78	46.88	27.34
O1/4	32.03	39.84	28.13	31.25	45.31	23.44	5.47	10.16	84.38*	6.25	11.72	82.03*	21.09	44.53	34.38	25.78	37.50	36.72
O1/5	53.91	33.59	12.50	52.34	34.38	13.28	22.66	37.50	39.84	27.34	25.78	46.88	21.09	41.41	37.50	25.78	45.31	28.91
O2/3	42.97	40.63	16.41	45.31	35.94	18.75	16.41	30.47	53.13*	26.56	25.00	48.44	33.59	51.56	14.84	32.81	51.56	15.63
O2/4	43.75	25.78	30.47	35.16	44.53	20.31	7.81	16.41	75.78*	9.38	21.88	68.75*	47.66	42.19	10.16	38.28	43.75	17.97
O2/5	43.75	35.16	21.09	48.44	41.41	10.16	13.28	21.09	65.63*	13.28	37.50	49.22	30.47	50.00	19.53	29.69	46.09	24.22
O3/4	34.38	35.16	30.47	38.28	39.84	21.88	5.47	18.75	75.78*	5.47	7.03	87.50*	26.56	53.13	20.31	34.38	50.00	15.63
O3/5	40.63	41.41	17.97	41.41	40.63	17.97	24.22	30.47	45.31	20.31	26.56	53.13*	37.50	51.56	10.94	40.63	51.56	7.81
O4/5	53.13	33.59	13.28	48.44	42.19	9.38	4.69	9.38	85.94*	3.13	6.25	90.63*	22.66	52.34	25.00	22.66	55.47	21.88

*$>50\%$ of precision values >1 mm, O: observer

The CBCT scans of patients were collected retrospectively. No age limitation was set in the study's inclusion criteria, although age may be a factor that causes variation in the sella turcica region. The inclusion criteria required that there be no abnormalities in the sella and sphenoidal regions, as previously published studies have shown that bridging of the sella turcica or calcification of the interclinoid ligament occurs in 1.1%-13% of the normal population.[24-26] This aspect of the inclusion criteria also implies that the system developed in the present study should only be used in patients without sella variations.

Bony resorption of the posterior part of the sella turcica may occur, potentially making it difficult to identify the border of the sella. The results of this study showed that for some landmarks (APT-L, APT-R, Sella 1, and Stella 2), the precision was subject-sensitive. One potential reason for this is of the possibility that the landmarks and bony structures were more difficult to visualize in the CBCT scans of some patients, and moreover, that image noise was more of a problem in some CBCTs.

The selection of the devices used to perform CBCT may also be a key factor in performing 3D cephalometry, as the choice of imaging device may affect the image quality and the quality of the 3D computed surface model. In the present study, the data were retrospectively collected and only one type of device was used. The CBCT data were tested for compatibility with the Maxilim® software.

The Maxilim® software showed a minor limitation in the segmentation of 3D surface models; namely, the software does not allow the operator to reduce any noise or artifacts in the image. Thus, some unwanted soft tissue parts and artifacts were included in the 3D model when the hard tissue threshold was selected to create a surface model. This caused some difficulties for the observers in viewing the images of patients whose CBCT images showed more noise and artifacts.

The reference system created in this study was comprised of four operator-indicated landmarks, two software-calculated landmarks, and two sella landmarks on two different vertical planes (Table 1). The landmarks used in the system were carefully selected to facilitate the precise identification of the center of the pituitary fossa. The landmarks forming the vertical planes were chosen because they are located adjacent to the sella turcica. Therefore, the vertical planes were not affected by variation in other craniofacial structures.

In this study, an upper limit of 1 mm was chosen as a clinical relevance level. No scientific evidence has shown that 1 mm is the optimal clinical standard. However, it is

usually presumed that larger differences may cause an unacceptable difference in measurements, potentially altering the results of cephalometric analysis.[20,27]

The results of this study showed that both the intraobserver and interobserver precision of all landmarks were moderate to very good. However, the precision was poorer for some landmarks (APT-R and APT-L), an effect that was most clearly seen in the interobserver precision results. Nonetheless, the poorer precision for these landmarks did not significantly alter the identification of the sella points on the corresponding vertical planes.

Intraobserver precision was slightly better than interobserver precision. This trend was expected, as differences between examiners are a factor that may influence the results of observational studies. Differences in the observers' backgrounds, their familiarity with the software, and their ability to identify landmarks according to the definitions provided all might affect interobserver precision. A calibration session was performed in order to minimize this effect as much as possible.

In this study, two of the observers (observers 1 and 2) had more experience in using the Maxilim® software before the observations. This led to a visible difference in the results. There were significant differences in intraobserver precision among observers for some landmarks (ACP-R, ACP-L, APT-R, and APT-L), and it was found that two observers (observers 1 and 2) were able to identify the landmarks more precisely. Moreover, significant differences between each pair of observers were found for all anatomical landmarks, implying that interobserver precision was observer-dependent. These findings may indicate that more calibration sessions should be performed in future studies assessing new software, or that observers should be selected based on their experience when it is possible to do so.

The overall reproducibility of all landmarks was satisfactory. The ACP-R and ACP-L were the most reproducible, followed by the two sella landmarks. The least reproducible landmarks were the APT-R and APT-L, showing the highest percentages of precision values >1 mm. The choice of using Sella 1 or Sella 2 made no significant difference. However, it is recommended to use Sella 2, established on the vertical plane which passes through a midpoint between the APT-R and APT-L, because the ACP-R and ACP-L points were more reproducible and therefore are preferable to be used independently.

Some previous studies have reported 3D landmark reproducibility results, using a range of methods. However, no sella-specific reference system similar to that presented in this study has been evaluated previously. Therefore, the results of previous studies cannot be directly compared with the results from the present study.

In 2008, Marumatsu et al.[28] reported the plotting reproducibility of landmarks on 3D CT using the 95% confidence ellipse method. The methodology of this study differed from that of the present study, as the landmarks were located only on axial CT images of one phantom head. Some variation was reported in the reproducibility of the sella turcica.[28]

Another study was conducted by de Oliveira et al.[23] to evaluate 3D landmark identification. The results showed a high intraclass correlation coefficient for both intraobserver and interobserver assessments. The authors concluded that 3D landmark identification using CBCT could offer reproducible data, if a protocol for operator training and calibration was followed.[23] In the present study, a calibration session was carried out, and the landmarks were carefully defined.

Hassan et al.[29] have suggested that landmark identification can be improved by using both multiplanar reconstruction images and 3D models, as some errors may occur during the segmenting process of 3D surface models. Thus, using 3D surface models with confirmation from multiplanar reconstruction images may help decrease segmenting-related errors, consequently increasing the accuracy of landmark identification.

In orthodontics, the sella point is utilized as a reference for evaluating the longitudinal growth of patients and to evaluate the results of treatment. It is be used as a reference point by superimposing several lateral cephalograms and comparing angles (e.g., comparing the sella-nasion-point A angle or the sella-nasion-point B angle). Further studies should be conducted in order to integrate this sella reference system into 3D cephalometric analysis and to assess how this system may influence the angular measurements and the results of multiple 3D cephalometric analyses.

The sella turcica landmark is one of the most important cephalometric landmarks, although it is a floating landmark in nature. A newly developed reference system offers high precision and reproducibility in identifying the sella point in a 3D model, without being based on 2D images derived from 3D data.

Acknowledgments

The authors would like to thank Ellen Ghijselings and Sophie Carpentier, who participated in the observations.

References

1. Alkofide EA. Sella turcica morphology and dimensions in cleft subjects. Cleft Palate Craniofac J 2008; 45: 647-53.
2. Axelsson S, Storhaug K, Kjaer I. Post-natal size and morphology of the sella turcica. Longitudinal cephalometric standards for Norwegians between 6 and 21 years of age. Eur J Orthod 2004; 26: 597-604.
3. Brock-Jacobsen MT, Pallisgaard C, Kjaer I. The morphology of the sella turcica in monozygotic twins. Twin Res Hum Genet 2009; 12: 598-604.
4. Kjær I. Sella turcica morphology and the pituitary gland - a new contribution to craniofacial diagnostics based on histology and neuroradiology. Eur J Orthod 2015; 37: 28-36.
5. Teal JS. Radiology of the adult sella turcica. Bull Los Angeles Neurol Soc 1977; 42: 111-74.
6. Alkofide EA. The shape and size of the sella turcica in skeletal Class I, Class II, and Class III Saudi subjects. Eur J Orthod 2007; 29: 457-63.
7. Andredaki M, Koumantanou A, Dorotheou D, Halazonetis DJ. A cephalometric morphometric study of the sella turcica. Eur J Orthod 2007; 29: 449-56.
8. Hofrath H. Bedeutung der Röntgenfern und Abstands Aufnahme für die Diagnostik der Kieferanomalien. Fortschr Orthod 1931; 1: 231-58.
9. Broadbent BH. A new x-ray technique and its application to orthodontia. Angle Orthod 1931; 1: 45-66.
10. Pauwels R, Beinsberger J, Collaert B, Theodorakou C, Rogers J, Walker A, et al. Effective dose range for dental cone beam computed tomography scanners. Eur J Radiol 2012; 81: 267-71.
11. Mah JK, Huang JC, Choo H. Practical applications of cone-beam computed tomography in orthodontics. J Am Dent Assoc 2010; 141: 7S-13S.
12. Kau CH, Richmond S, Palomo JM, Hans MG. Three-dimensional cone beam computerized tomography in orthodontics. J Orthod 2005; 32: 282-93.
13. van Vlijmen OJ, Kuijpers MA, Bergé SJ, Schols JG, Maal TJ, Breuning H, et al. Evidence supporting the use of cone-beam computed tomography in orthodontics. J Am Dent Assoc 2012; 143: 241-52.
14. Swennen GR, Schutyser F, Barth EL, De Groeve P, De Mey A. A new method of 3-D cephalometry Part I: the anatomic Cartesian 3-D reference system. J Craniofac Surg 2006; 17: 314-25.
15. Olszewski R, Cosnard G, Macq B, Mahy P, Reychler H. 3D CT-based cephalometric analysis: 3D cephalometric theoretical concept and software. Neuroradiology 2006; 48: 853-62.
16. Periago DR, Scarfe WC, Moshiri M, Scheetz JP, Silveira AM, Farman AG. Linear accuracy and reliability of cone beam CT derived 3-dimensional images constructed using an orthodontic volumetric rendering program. Angle Orthod 2008; 78: 387-95.
17. Brown AA, Scarfe WC, Scheetz JP, Silveira AM, Farman AG. Linear accuracy of cone beam CT derived 3D images. Angle Orthod 2009; 79: 150-7.
18. Olszewski R, Tanesy O, Cosnard G, Zech F, Reychler H. Reproducibility of osseous landmarks used for computed tomography based three-dimensional cephalometric analyses. J Craniomaxillofac Surg 2010; 38: 214-21.
19. Olszewski R, Frison L, Wisniewski M, Denis JM, Vynckier S, Cosnard G, et al. Reproducibility of three-dimensional cephalometric landmarks in cone-beam and low-dose computed tomography. Clin Oral Investig 2013; 17: 285-92.
20. Pittayapat P, Limchaichana-Bolstad N, Willems G, Jacobs R. Three-dimensional cephalometric analysis in orthodontics: a systematic review. Orthod Craniofac Res 2014; 17: 69-91.
21. Schlicher W, Nielsen I, Huang JC, Maki K, Hatcher DC, Miller AJ. Consistency and precision of landmark identification in three-dimensional cone beam computed tomography scans. Eur J Orthod 2012; 34: 263-75.
22. Chien PC, Parks ET, Eraso F, Hartsfield JK, Roberts WE, Ofner S. Comparison of reliability in anatomical landmark identification using two-dimensional digital cephalometrics and three-dimensional cone beam computed tomography in vivo. Dentomaxillofac Radiol 2009; 38: 262-73.
23. de Oliveira AE, Cevidanes LH, Phillips C, Motta A, Burke B, Tyndall D. Observer reliability of three-dimensional cephalometric landmark identification on cone-beam computerized tomography. Oral Surg Oral Med Oral Pathol Oral Radiol Endod 2009; 107: 256-65.
24. Meyer-Marcotty P, Reuther T, Stellzig-Eisenhauer A. Bridging of the sella turcica in skeletal Class III subjects. Eur J Orthod 2010; 32: 148-53.
25. Cederberg RA, Benson BW, Nunn M, English JD. Calcification of the interclinoid and petroclinoid ligaments of sella turcica: a radiographic study of the prevalence. Orthod Craniofac Res 2003; 6: 227-32.
26. Bergland RM, Ray BS, Torack RM. Anatomical variations in the pituitary gland and adjacent structures in 225 human autopsy cases. J Neurosurg 1968; 28: 93-9.
27. Durão AR, Pittayapat P, Rockenbach MI, Olszewski R, Ng S, Ferreira AP, et al. Validity of 2D lateral cephalometry in orthodontics: a systematic review. Prog Orthod 2013; 14: 31.
28. Muramatsu A, Nawa H, Kimura M. Reproducibility of maxillofacial anatomic landmarks on 3-dimensional computed tomographic images determined with the 95% confidence ellipse method. Angle Orthod 2008; 78: 396-402.
29. Hassan B, Nijkamp P, Verheij H, Tairie J, Vink C, van der Stelt P, et al. Precision of identifying cephalometric landmarks with cone beam computed tomography in vivo. Eur J Orthod 2013; 35: 38-44.